Flight data reduction methodology for performance evaluation and comparison of model-following adaptive control laws

M. G. Perhinschi and M. R. Napolitano
Department of Mechanical and Aerospace Engineering
West Virginia University, Morgantown
West Virginia, USA

ABSTRACT

Even small differences in atmospheric and/or flight conditions can potentially impact significantly the evaluation of the performance of the control laws and prevent a correct comparison, especially in the case of reduced size aircraft (autonomous or remotely piloted). Consistent deterministic control inputs can only be guaranteed through some form of computer-based on-board excitation system. In this paper, a methodology is proposed for flight data reduction with the purpose of accounting for non-homogeneous atmospheric conditions and inconsistent pilot inputs. The method is developed for the specific purpose of comparing model-following adaptive control laws. Performance evaluation parameters based on angular rate tracking errors are defined and used for the comparison. As a result of this approach, an additive correction is applied to the angular rate measurements to compensate for non-homogeneous turbulence effects. A multiplicative correction factor is applied to the angular rate tracking error to take into account non-identical pilot inputs. The procedure is validated with simulation and flight data obtained in the process of designing a set of fault tolerant control laws based on non-linear dynamic inversion with neural network augmentation for the reduced size WVU YF-22 aircraft model.

NOMENCLATURE

d	duration of doublet input
DR	data reduction
EP	evaluation parameter
ITE	integral of the absolute value of the tracking error
K	correction factor
LPF	low pass filter
$MXTE$	maximum of the absolute value of the tracking error
n	number of samples
$NLDI$	non-linear dynamic inversion
NN	neural network
p, q, r,	angular rates
$P1$, $P2$…	test identifier for different pilot input
RPV	remotely piloted vehicles
s	Laplace variable
STD	standard deviation
t	time
$T1$, $T2$…	test identifier for different turbulence level
TE	tracking error
TF	transfer function
u	aircraft controls
UAV	unmanned aerial vehicle
WVU	West Virginia University
x	aircraft states
δ	control surface deflection
Δ	gradient
σ	standard deviation
τ	time constant
ω	natural frequency
ζ	damping ratio

Paper No. 3221. Manuscript received 18 July 2007, accepted 5 November 2007.

https://doi.org/10.1017/S0001924000001925 Published online by Cambridge University Press

Subscripts

A	first set of control laws in the comparison
act	sensor output
A/C	aircraft
B	second set of control laws in the comparison
com	command
Cont	controller model
err	error
HQ	reference model
ref	reference model
Sens	sensor model
st	pilot stick
t	turbulence
Z	controlled system model

Superscripts

(*PC*)	correction for pilot input
(*TC*)	correction for turbulence

1.0 INTRODUCTION

The measurement of aircraft performance in flight tests provides the ultimate assessment of its capability to fulfill its role as expected. The need for the evaluation parameters to be determined under identical conditions – for any comparison to be pertinent – is a truism. Standard conditions have been defined for numerous dynamic performance parameters (e.g. maximum speed, ceiling, climb rate, etc.) and algorithms are available to compute equivalent values when the measurements are taken under non-standard conditions[1,2]. Handling qualities assessment related to the development of advanced flight control laws poses additional challenges. In fact, analytical parameters and criteria are difficult to define and the whole process relies by definition on the subjective evaluation of human pilots. Standard procedures are defined for manned aircraft[3]. However, a similar set of procedures does not exist for remotely piloted vehicles (RPV).

Due to high risks and increasing costs of full size aircraft flight testing, the use of research RPVs emerges as a promising alternative for supporting the design and development of advanced flight control laws. Low cost scale aerial platforms have been extensively used at West Virginia University (WVU) for data acquisition, parameter identification, and testing of control laws for specific flight control problems[4-6]. Model following control schemes[7,8] – for which the minimisation of the tracking errors (TE) is a natural criterion for performance evaluation – have received substantial attention for a variety of control applications. In particular, adaptive control schemes based on non-linear dynamic inversion (NLDI) – augmented with neural networks (NN) for the cancellation of residual dynamic inversion errors – have been extensively used in recent years[6,9,10]. This class of control laws has shown to provide desirable handling qualities without requiring the level of computational effort associated with other approaches based on gain-scheduling and/or system identification; however, extensive flight testing is still needed. Based on this control architecture, research activities at WVU were aimed at designing and flight testing fault tolerant NLDI+NN control laws using YF-22 aircraft scale models[6]. The specific characteristics of designing and operating unmanned aerial vehicles (UAVs), including flight testing, have been acknowledged[11,12] within the professional community.

The performance of different flight control laws can be evaluated and compared if appropriate evaluation parameters are defined and determined under identical test conditions. While this is always possible for numerical simulations, in general it can not be achieved for actual flight tests. In this paper, an algorithm is developed for flight data reduction to account for different atmospheric conditions and pilot input dissimilarities. Small differences in atmospheric conditions can potentially impact significantly the evaluation of controller performance and prevent consistent comparison especially in the case of reduced size aircraft (autonomous or remotely piloted). Slightly different pilot input can not be avoided if an automated system is not available and/or the test must extend over longer periods of time, thus leading to different dynamic responses.

In the next section, the general architecture of a set of neurally augmented dynamic inversions-based control laws is briefly described. The specific problem of comparing the performance of different control laws within the model-following category is formulated in Section 3. Data correction algorithms are proposed in Section 4 to address the issues of dissimilar atmospheric conditions and in Section 5, for dissimilar pilot inputs. The WVU YF-22 simulator of a research RPV is used to verify the approach. Results are presented and discussed in Section 6. Data acquired during the flight testing of the reduced size WVU YF22 aircraft are used to illustrate the application of the proposed methodology in Section 7. The WVU YF-22 aircraft has a wingspan of 1·98m, a maximum take-off weight of 214N, and is equipped with a jet engine providing a maximum thrust of 125N.

2.0 ARCHITECTURE OF THE CONTROL LAWS

The model-following control concept is based on the idea that desirable performance and handling qualities can be obtained if the control laws produce aircraft responses similar to responses from pre-determined models, called command or reference models. Let the dynamics of the aircraft be described by the following nonlinear system of equations:

$$\dot{x} = f(x,u) \qquad \ldots (1)$$

and the reference model be expressed in general as:

$$\dot{x}_{ref} = f_{ref}\left(x_{ref},u\right) \qquad \ldots (2)$$

For an RPV, the flight commands are generated by the pilot through the longitudinal, lateral, and directional stick ($\delta_{lon_{stick}}$, $\delta_{lat_{stick}}$ and $\delta_{dir_{stick}}$). These displacements are first converted into corresponding state commands within the 'command shaping' block, as shown in Fig. 1. Note that the proposed methodology can be applied to a variety of state command selections with appropriate adaptation. However, for the purpose of this effort, the commanded states will be considered to be the roll, pitch, and yaw rate (p_{com}, q_{com}, r_{com}). Typically, reference models have been developed for airplanes as first and/or second order linear systems based on handling qualities requirements[3,13]. Therefore, including the command shaping, Equation (2) becomes:

$$p_{ref}(s) = \frac{1}{s+\tau_{roll}}\, p_{com}(s)$$

$$q_{ref}(s) = \frac{\omega^2_{n_{pitch}}}{s^2 + 2\zeta_{pitch}\omega_{n_{pitch}} + \omega^2_{n_{pitch}}}\, q_{com}(s) \qquad \ldots (3)$$

$$r_{ref}(s) = \frac{\omega^2_{n_{yaw}}}{s^2 + 2\zeta_{yaw}\omega_{n_{yaw}} + \omega^2_{n_{yaw}}}\, r_{com}(s)$$

The tracking error (TE) can be determined on all three channels based on the reference values and sensor output as:

$$\text{TE} = x_{ref} - x_{act} \text{ where } x = p, q \text{ or } r \qquad \ldots (4)$$

The data reduction methodology proposed in this paper can be applied to control laws of various structures. However, the methodology was developed as part of a research effort with the objective of assessing and comparing through flight testing the fault tolerant capabilities from different classes of NNs within a particular architecture. This architecture included a proportional and integral compensator, an inversion process, and neural augmentation as shown in Fig. 1. More details about the control laws can be found in Ref. 6.

https://doi.org/10.1017/S0001924000001925 Published online by Cambridge University Press

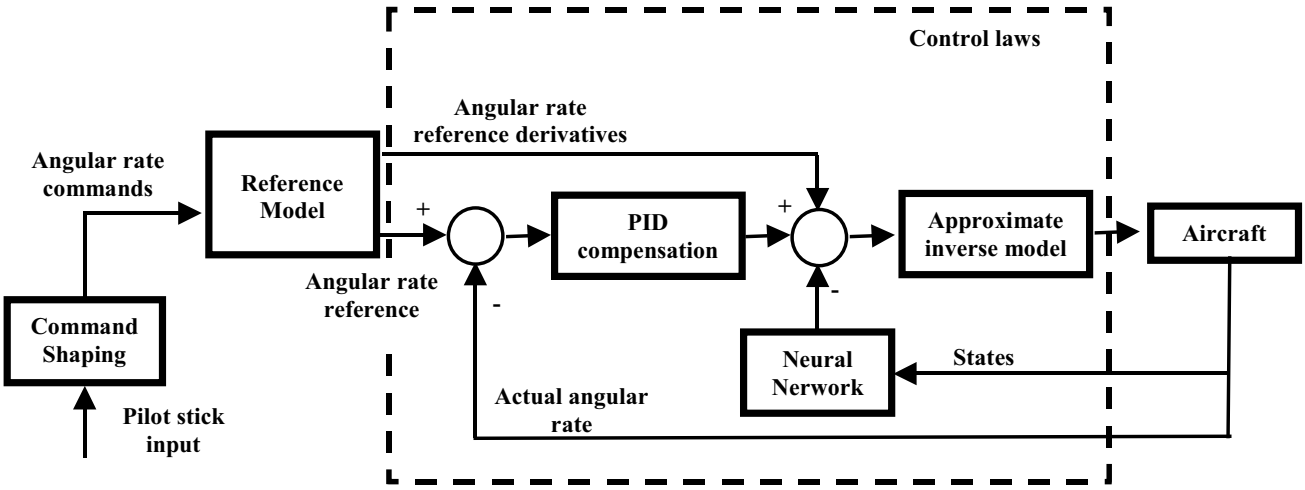


Figure 1. General scheme of the NLDI+NN control laws.

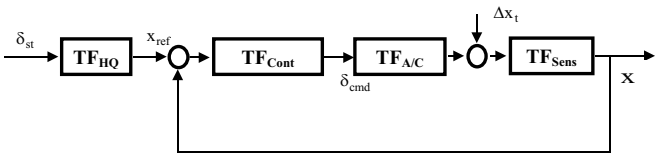


Figure 2. Approximate representation of the controlled aircraft system.

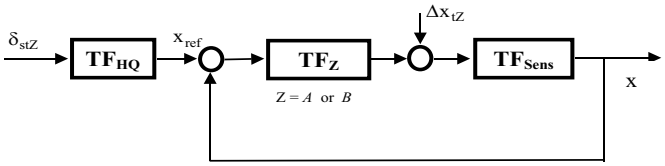


Figure 3. Approximate compact representation of the controlled aircraft system.

3.0 PERFORMANCE COMPARISON OF CONTROL LAWS – PROBLEM DESCRIPTION AND ASSUMPTIONS

The main objective of the flight tests was to support the analysis of the control laws performance and the comparison between different versions. In particular, the goal was to assess the contribution of the NN within the NLDI+NN control laws relative to the baseline version using only NLDI. In general, a set of control laws *A* is compared against a different set *B* within the same structural class. Given the model-following type of architecture, the performance evaluation parameters used in the comparison are based on the angular rates TEs computed as difference between the reference and measured (actual) values according to Equation (4). These TEs and their statistics depend on the specific flight conditions (including atmospheric turbulence) and the pattern, magnitude, and duration of the pilot inputs. All these elements must be identical for the comparison to be pertinent. The comparison is made in terms of the standard deviation (STD) of the angular rate TE, the integral of the TE, and the maximum value of the absolute value of the angular rate TE.

An attempt was made to perform flight testing sessions under similar atmospheric conditions. However, differences in atmospheric perturbations were unavoidable from one day to an other or even within the same flight session. Nevertheless, small variations may have a significant impact on the evaluation parameters due to the reduced size of the aircraft and its low speed.

For each of the flight tests, the pilots were required to perform doublets on all three channels. Although they were able to repeat the general pattern of the input, the magnitude and the duration of the maneuvers could not be identical. Therefore, a post-flight procedure was needed to compare the results from different flights[14] and/or different maneouvers with similar patterns. The differences in the general test conditions were assessed in terms of specific 'evaluation parameters' (EP). The EPs considered were:

- standard deviation of the perturbations attributed to atmospheric turbulence;
- integral of the absolute value of the pilot input.

The approach consists of 'correcting' the set of data corresponding to control laws *A* (one element of the comparison) in such a way as to obtain a set of data with an EP equal to the one of the second element of comparison – the data corresponding to control laws *B*. Assuming superposition of effects, two types of corrections were determined, that is an additive correction to account for different atmospheric conditions and a multiplicative correction to account for dissimilar pilot inputs.

Let us denote with $\hat{x}(t)$ the time histories of measured angular rates for segments were there is no pilot input and the controller is turned off. Let $\sigma(x)$ be the STD of x. With these notations, the following additional assumptions were used in the development of the data reduction algorithm:

1. The statistical characteristics of atmospheric turbulence are constant for the duration of any given test although they may vary from one test session to an other.
2. $\sigma(\hat{x})$ is a measurement of the turbulence level.
3. The average of $\sigma(\hat{x})$ over several segments is a measure of turbulence for segments with non-zero pilot input during the same flight and is equal to the STD of the perturbations due to turbulence.
4. The system can be modeled through the block diagram of Fig. 2 where all the transfer functions exist and are valid representations/approximations of the respective systems. Moreover, compact representations of the system including the control laws sets *A* and *B* exist, as described in Fig. 3. Note that only the existence and not the computation of the transfer functions involved in these models is required. The notations in Figs 2 and 3 have the following meaning:

https://doi.org/10.1017/S0001924000001925 Published online by Cambridge University Press

TF_{HQ} = first or second order reference model
$TF_{A/C}$ = approximation of aircraft dynamics
TF_{Cont} = approximation of the control laws
TF_{Z} = compact approximation of the controlled system
TF_{Sens} = sensor model
δ_{st} = pilot input
Δx_t = perturbation due to atmospheric turbulence
x = measured angular rate (p, q, or r)

Based on these assumptions, the measured angular rates can be expressed as:

$$x_Z(s) = TF_{HQ}(s)\frac{TF_Z(s)\cdot TF_{Sens}(s)}{1+TF_Z(s)\cdot TF_{Sens}(s)}\delta_{stZ}(s) + \frac{TF_{Sens}(s)}{1+TF_Z(s)\cdot TF_{Sens}(s)}\Delta x_Z(s) \quad \ldots (5)$$

Note that Z can take the values A or B depending on the specific set of control laws being tested. For compactness purposes, the following substitution will be used next:

$$TF_{ZS}(s) = TF_Z(s)\cdot TF_{Sens}(s) \quad \ldots (6)$$

The reference values of the angular rates can be represented by the relationship:

$$x_{refZ}(s) = TF_{HQ}(s)\delta_{stZ}(s) \quad \ldots (7)$$

The resulting angular rate TEs can be expressed as:

$$x_{errZ}(s) = x_{refZ}(s) - x_Z(s) = TF_{HQ}(s)\left[1-\frac{TF_{ZS}(s)}{1+TF_{ZS}(s)}\right]\delta_{stZ}(s) - \frac{TF_{Sens}(s)}{1+TF_{ZS}(s)}\Delta x_Z(s) \quad \ldots (8)$$

4.0 DATA CORRECTION TO ACCOUNT FOR NON-HOMOGENEOUS ATMOSPHERIC CONDITIONS

The STD of the measured angular rates relative to segments were there is no pilot input and the controller is off, for case A (e.g. NLDI-only control laws), is expressed as:

$$\sigma(\hat{x}_A(t)) = \sqrt{\sum_i^n (\hat{x}_{Ai} - \bar{\hat{x}}_A)^2/(n-1)} \quad \ldots (9)$$

where the *bar* notation is used for the mean and n is the number of samples. The corresponding STD for flight test B (e.g. NLDI+NN control laws) is given by:

$$\sigma(\hat{x}_B(t)) = \sqrt{\sum_i^n (\hat{x}_{Bi} - \bar{\hat{x}}_B)^2/(n-1)} \quad \ldots (10)$$

Let us denote the ratio of the two STDs by:

$$K_{t1} = \frac{\sigma(\hat{x}_B(t))}{\sigma(\hat{x}_A(t))} \quad \ldots (11)$$

It can be shown that:

$$\sigma(K_{t1}\cdot\hat{x}_A(t)) = \sigma(\hat{x}_B(t)) \quad \ldots (12)$$

To prove this statement, Equation (9) is used first to obtain:

$$\sigma(K_{t1}\hat{x}_A(t)) = \sqrt{\sum_{i=1}^n (K_{t1}\cdot\hat{x}_A - \overline{(K_{t1}\cdot\hat{x}_A)})^2/(n-1)} \quad \ldots (13)$$

Based on the linearity of the mean operator, after a few simple manipulations, and using Equation (11), we obtain:

$$\sigma(K_{t1}\hat{x}_A(t)) = K_{t1}\sqrt{\sum_{i=1}^n (\hat{x}_A - \bar{\hat{x}}_A)^2/(n-1)} = K_{t1}\sigma(\hat{x}_A(t)) = \sigma(\hat{x}_B(t)) \quad \ldots (14)$$

The processed data can also be expressed as:

$$K_{t1}\cdot\hat{x}_A(t) = \hat{x}_A(t) + \Delta\hat{x}_t(t) \quad \ldots (15)$$

where:

$$\Delta\hat{x}_t(t) = (K_{t1}-1)\hat{x}_A(t) \quad \ldots (16)$$

In other words, adding the quantity $\Delta\hat{x}_t(t)$ to $\hat{x}_A(t)$ one can achieve a similarity conversion from the level of atmospheric turbulence recorded during test A to the level of atmospheric turbulence of test B. The next step is to apply such a correction to the measurements of the state variable $x_A(t)$. Converting $x_A(t)$ into $x_A^{(TC)}(t)$ to account for different atmospheric conditions implies that only the term representing the contribution of the turbulence will be affected; therefore:

$$x_A^{(TC)}(s) = TF_{HQ}(s)\frac{TF_{AS}(s)}{1+TF_{AS}(s)}\delta_{stA}(s) + \frac{TF_{Sens}(s)}{1+TF_{AS}(s)}\Delta x_{tA}^{(TC)}(s) \quad \ldots (17)$$

where $\Delta x_{tA}^{(TC)}$ must meet the requirement:

$$\sigma(\Delta x_{tA}^{(TC)}(t)) = \sigma(\Delta x_{tB}(t)) \quad \ldots (18)$$

$\Delta x_{tA}^{(TC)}(t)$ can be evaluated using the relationship:

$$\Delta x_{tA}^{(TC)}(t) = \Delta x_{tA}(t) + K_{t2}\cdot\Delta\hat{x}_t(t) \quad \ldots (19)$$

where K_{t2} is a correction factor that must be determined such that:

$$\sigma(K_{t2}\Delta\hat{x}_t + \Delta x_{tA}) = \sigma(\hat{x}_B) \quad \ldots (20)$$

Since $\Delta x_{tA}(t)$ and $\Delta\hat{x}_t(t)$ are uncorrelated, Equation (20) can be written as:

$$K_{t2}^2\cdot\sigma^2(\Delta\hat{x}_t) + \sigma^2(\Delta x_{tA}) = \sigma^2(\hat{x}_B) \quad \ldots (21)$$

According to assumption #3:

$$\sigma(\Delta x_{tA}) = \sigma(\hat{x}_A) \quad \ldots (22)$$

For $\sigma(\hat{x}_B) > \sigma(\hat{x}_A)$, the following expression for the correction factor can be obtained:

$$K_{t2}^2 = \frac{\sigma(\hat{x}_B)+\sigma(\hat{x}_A)}{\sigma(\hat{x}_B)-\sigma(\hat{x}_A)} \quad \ldots (23)$$

Using Equation (19), Equation (17) can now be written as:

$$x_A^{(TC)}(s) = TF_{HQ}(s)\frac{TF_{AS}(s)}{1+TF_{AS}(s)}\delta_{stA}(s) + \frac{TF_{Sens}(s)}{1+TF_{AS}(s)}\Delta x_{tA}(s) + K_{t2}\frac{TF_{Sens}(s)}{1+TF_{AS}(s)}\Delta\hat{x}_t(s) \quad \ldots (24)$$

Therefore, the corrected measurement to take into account differences in the atmospheric conditions can be expressed as:

$$x_A^{(TC)}(t) = x_A(t) + K_{t2}\cdot\Delta\hat{x}_t(t) \quad \ldots (25)$$

5.0 DATA CORRECTION TO ACCOUNT FOR DISSIMILAR PILOT INPUTS

The angular rates TE after the 'turbulence correction' can be expressed as:

$$x_{errA}^{(TC)}(s) = x_{refA}(s) - x_A^{(TC)}(s) = TF_{HQ}(s)\left[1+\frac{TF_{AS}(s)}{1+TF_{AS}(s)}\right]\delta_{stA}(s) + \quad \ldots (26)$$

https://doi.org/10.1017/S0001924000001925 Published online by Cambridge University Press

$$+\frac{TF_{Sens}(s)}{1+TF_{AS}(s)}\Delta x_{tA}^{(TC)}(s)$$

Assume that a low-pass filtered $x_{errA}^{(TC)}(s)$ is equal to:

$$LPF[x_{errA}^{(TC)}(s)] = TF_{HQ}(s)\left[1+\frac{TF_{AS}(s)}{1+TF_{AS}(s)}\right]\delta_{stA}(s) \quad \ldots (27)$$

In other words, assume that the filtering separates that part of the pilot input contribution on which we want to perform the correction. Let us denote:

$$\Delta x_{errA}^{*}(s) = x_{errA}^{(TC)}(s) - LPF[x_{errA}^{(TC)}(s)] \quad \ldots (28)$$

A corrected TE to account for pilot input differences can then be expressed as:

$$x_{errA}^{(PC)}(s) = x_{errA}^{(PC*)}(s) + \Delta x_{errA}^{*}(s) \quad \ldots (29)$$

where the correction is the result of a modified pilot input $\delta_{stA}^{(PC)}(s)$:

$$x_{errA}^{(PC*)}(s) = TF_{HQ}(s)\left[1+\frac{TF_{AS}(s)}{1+TF_{AS}(s)}\right]\delta_{stA}^{(PC)}(s) \quad \ldots (30)$$

therefore:

$$x_{errA}^{(PC)}(s) = TF_{HQ}(s)\left[1+\frac{TF_{AS}(s)}{1+TF_{AS}(s)}\right]\delta_{stA}^{(PC)}(s) + \Delta x_{errA}^{*}(s) \quad \ldots (31)$$

where the corrected pilot input $\delta_{stA}^{(PC)}(s)$ is such that:

$$\int\left|\delta_{stA}^{(PC)}(t)\right|dt = \int\left|\delta_{stB}(t)\right|dt \quad \ldots (32)$$

Assuming $K_{pilot1} = \dfrac{\int|\delta_{stB}(t)|dt}{\int|\delta_{stA}(t)|dt}$, then:

$$x_{errA}^{(PC)}(s) = LPF[x_{errA}^{(TC)}(s)]\cdot K_{pilot1}\cdot K_{pilot2} + \Delta x_{errA}^{*}(s) \quad \ldots (33)$$

The correction factor K_{pilot2} takes into account that changes of the pilot input integral due to changes in the magnitude have a more significant effect on the TE than changes due to variation of the duration. It was determined from simulations that K_{pilot2} can be expressed as the ratio of the durations of the two doublet inputs:

$$K_{pilot2} = \frac{d_A}{d_B} \quad \ldots (34)$$

The correction for pilot input dissimilarities can be expressed in the time domain as:

$$x_{errA}^{(PC)}(t) = LPF[x_{errA}^{(TC)}(t)]\cdot K_{pilot1}\cdot K_{pilot2} + \Delta x_{errA}^{*}(t) \quad \ldots (35)$$

6.0 VERIFICATION OF THE PROPOSED APPROACH THROUGH NUMERICAL SIMULATION

For the verification of the proposed data reduction methodology, a series of 15 seconds simulation tests was designed using the WVU YF-22 Simulator[15]. A set of longitudinal and lateral stick doublet inputs were considered, as shown in Fig. 4, with the following characteristics:

*P*1 = nominal magnitude to produce a ±3 degrees control surface deflection over 2·5 seconds;
*P*2 = 0·75 × nominal magnitude over 2·5 seconds;

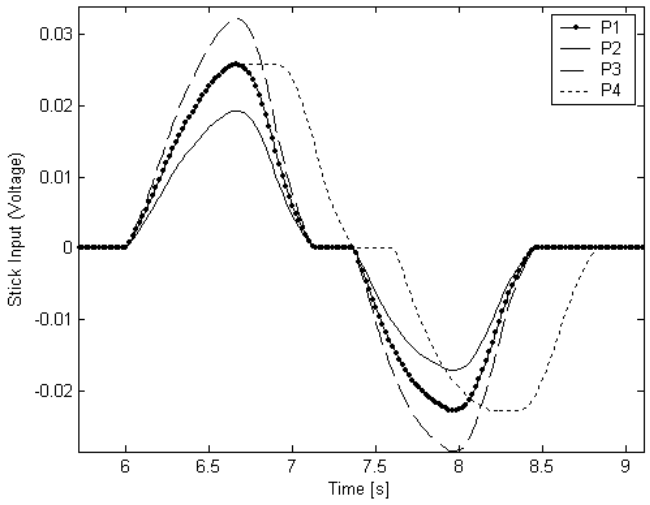


Figure 4. Pilot inputs used for numerical simulation.

*P*3 = 1·25 × nominal magnitude 2·5 seconds;
*P*4 = nominal magnitude over 3 seconds.

The presence of atmospheric turbulence was simulated simultaneously on all three axes using the Dryden turbulence model with different values of the standard deviation of the air velocity :

*T*1 = σ_w = 1ms^{-1};
*T*2 = σ_w = 1·5ms^{-1};
*T*3 = σ_w = 2ms^{-1}.

Combining all possibilities, a total of 12 cases were simulated and compared to each other in terms of the following performance metrics:

STD = standard deviation of the roll and pitch rate TE, respectively;
ITE = integral of the absolute value of the roll and pitch rate TE, respectively;
MXTE = maximum of the absolute value of the roll and pitch rate TE, respectively.

In particular, the relative differences between the values of these parameters for control laws set A and B were used. For example:

$$\overline{STD} = \left|\frac{STD_A - STD_B}{STD_A}\right|\cdot 100\% \quad \ldots (36)$$

These parameters were computed before and after the application of the data reduction (DR) algorithm. Without loss of generality, the same set of control laws was compared against itself. In this case, the outcome of the comparison should ideally be that control laws set *A* has identical performance as control laws set *B*, or equivalently, the values of the comparison parameters are all zero. The control laws set used in this study was based on NLDI augmented with a single hidden layer NN[6].

Out of the total 792 individual comparison cases, an example is presented in Table 1 showing the relative differences of STD of the pitch rate TE, before and after the application of the DR algorithm, for all four pilot input types applied on the pitch channel, and under different turbulence conditions. It can be seen that the comparison based on raw data produces large differences between the evaluation parameters — up to 70% — where it should produce no difference since the two control laws sets are identical. The application of the DR algorithm reduces significantly this discrepancy.

To quantitatively assess the performance of the proposed methodology, the average relative differences of the three evaluation parameters were computed for various subsets of tests. These results

https://doi.org/10.1017/S0001924000001925 Published online by Cambridge University Press

Table 1
Relative difference in control laws performance evaluation parameters – before and after the application of the data reduction algorithm

[%]		P1T1	P2T1	P3T1	P4T1	P1T2	P2T2	P3T2	P4T2
P1T3	Before DR	13	41	8	11	6	31	12	7
	After DR	5	1	6	1	2	5	4	1
P2T3	Before DR	6	17	24	7	11	9	27	11
	After DR	11	6	12	7	9	2	11	6
P3T3	Before DR	34	68	10	33	27	56	5	28
	After DR	2	4	4	2	2	9	1	4
P4T3	Before DR	11	38	10	9	4	28	14	5
	After DR	6	1	8	2	3	4	6	1

Table 2
Average relative difference of the STD of angular rates TE – before and after the application of the data reduction algorithm

[%]		Overall		Only turbulence dissimilarities		Only pilot input dissimilarities		Simultaneous turbulence & pilot dissimilarities	
		Before	After	Before	After	Before	After	Before	After
Longitudinal input	Pitch rate TE	20	4	8	2	22	5	23	5
	Roll rate TE	37	3	37	3	-	-	37	3
Lateral input	Pitch rate TE	24	11	24	11	-	-	24	11
	Roll rate TE	20	5	7	2	23	5	24	5
All cases, pitch and roll rate TE		20	5	12	3	22	5	24	5

Table 3
Average relative difference of the integral of angular rates TE – before and after the application of the data reduction algorithm

[%]		Overall		Only turbulence dissimilarities		Only pilot input dissimilarities		Simultaneous turbulence & pilot dissimilarities	
		Before	After	Before	After	Before	After	Before	After
Longitudinal input	Pitch rate TE	16	7	12	3	16	9	18	8
	Roll rate TE	35	2	35	2	-	-	35	2
Lateral input	Pitch rate TE	24	10	24	10	-	-	24	10
	Roll rate TE	18	7	14	1	15	8	23	9
All cases, pitch and roll rate TE		18	7	16	3	15	9	22	8

Table 4
Average relative difference of the maximum of the angular rates TE — before and after the application of the data reduction algorithm

[%]		Overall		Only turbulence dissimilarities		Only pilot input dissimilarities		Simultaneous turbulence & pilot dissimilarities	
		Before	After	Before	After	Before	After	Before	After
Longitudinal input	Pitch rate TE	16	9	8	9	18	8	19	9
	Roll rate TE	37	11	37	11	-	-	37	11
Lateral input	Pitch rate TE	16	14	16	14	-	-	16	14
	Roll rate TE	20	6	2	7	25	2	24	8
All cases, pitch and roll rate TE		19	8	9	9	21	5	22	9

Table 5
Rate of success of the data reduction algorithm to correct performance evaluation based on the STD of angular rates TE

[%]		Overall	Only turbulence dissimilarities	Only pilot input dissimilarities	Simultaneous turbulence & pilot dissimilarities
Longitudinal input	Pitch rate TE	91	100	83	92
	Roll rate TE	100	100	-	100
Lateral input	Pitch rate TE	100	100	-	100
	Roll rate TE	94	100	100	89
All cases, pitch and roll rate TE		93	100	92	91

https://doi.org/10.1017/S0001924000001925 Published online by Cambridge University Press

Table 6
Rate of success of the data reduction algorithm to correct performance evaluation based on the integral of angular rates TE

[%]		Overall	Only turbulence dissimilarities	Only pilot input dissimilarities	Simultaneous turbulence & pilot dissimilarities
Longitudinal input	Pitch rate TE	70	100	61	64
	Roll rate TE	100	100	-	100
Lateral input	Pitch rate TE	100	100	-	100
	Roll rate TE	85	100	89	78
All cases, pitch and roll rate TE		78	100	75	73

Table 7
Rate of success of the data reduction algorithm to correct performance evaluation based on the maximum of the angular rates TE

[%]		Overall	Only turbulence dissimilarities	Only pilot input dissimilarities	Simultaneous turbulence & pilot dissimilarities
Longitudinal input	Pitch rate TE	68	33	83	72
	Roll rate TE	100	100	-	100
Lateral input	Pitch rate TE	67	67	-	67
	Roll rate TE	73	33	89	78
All cases, pitch and roll rate TE		71	37	86	76

are shown in Tables 2, 3, and 4 for the STD of the angular rates TE, integral of the TE, and maximum value of the TE, respectively. In average, for all cases simulated, the application of the DR algorithm produces a reduction of the evaluation discrepancy from 20% to 5% for STD, from 18% to 7% for ITE, and from 19% to 8% for MXTE. The 'success rate' of the algorithm was computed as the percentage of cases in which the application of the algorithm produced a reduction of the evaluation discrepancy. These results are presented in Tables 5, 6, and 7 for the three evaluation parameters. The success rate of the DR algorithm is 93% when applied to STD, 78% when applied to ITE, and 71% when applied to MXTE. The overall success rate is 81%. It should be noted that when applied to MXTE, the correction for turbulence inconsistencies performs poorly.

7.0 APPLICATION OF THE PROPOSED APPROACH TO FLIGHT DATA

The comparison between the performance of NLDI-only and NLDI+NN control laws on the WVU YF-22 aircraft model is used next to illustrate the application of the proposed DR algorithm to flight data. One ten-minute flight was performed for each of the control laws version. The trajectory consisted of two straight legs in opposite direction connected by two left turns within visual range. A total of nine loops were flown for each test. The controller was active on some portions of the trajectory and turned off on others. The pilot input consisted of longitudinal and lateral doublets starting from straight level steady state flight. As expected, for each test the atmospheric conditions were different; the pilot input pattern was similar but the actual execution was different.

For performance assessment purposes, one segment of the time history of the tracking error with NN is compared against one segment of equal duration without the NN in terms of the STD of the angular rate TE and maximum of the absolute value of the angular rate TE. The duration of each segment is six seconds. Three segments for each version have been considered and compared to each other for a total of nine comparisons. The absolute value of the pitch rate TEs corresponding to actual measurements is shown in Fig. 5. Corrections to account for different atmospheric conditions were applied to the data obtained with the NLDI-only control laws following the algorithm described in Section 4. The corrected data are presented in Fig. 5(b). The corrections are limited in magnitude because the ratio K_{tl} from Equation 11 was close to 1.

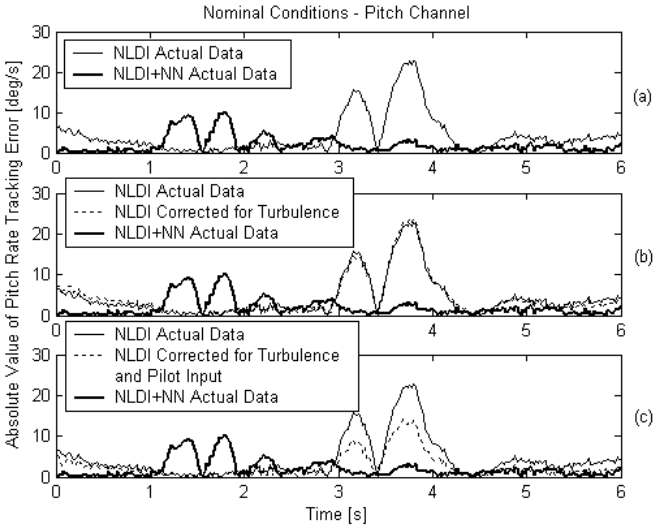


Figure 5. Data reduction effects on the absolute value of the pitch rate TE.

The dissimilarities in longitudinal pilot input can be assessed from Fig. 6(a). The equivalent (corrected) pilot input to ensure identical integral, as described in Section 5, is presented in Fig. 6(b). The corrected TEs after each step are shown in Figs 5(b) and 5(c). Significant changes of the evaluation parameters can be inferred from these plots due to the application of the DR algorithm. The corrected values of the TE were used to determine the STD and the maximum as performance evaluation and comparison parameters. These parameters for each of the three cases considered for the NLDI-only version are compared against the parameters for each of the three cases considered for the NLDI+NN version and percentage reductions – as a result of NN activity – are computed. Table 8 presents the percentage reduction of the STD and maximum of pitch rate TE produced by the activity of the NN within the control laws. Negative values for the parameters in Table 8 were used to represent percentage increases. The data presented in Figs 5 and 6 are relative to Case #3 of the NLDI+NN control laws and Case #2 of the NLDI-only control laws from Table 8. The effect of the NN augmentation can be assessed using the average reduction produced on the evaluation parameter over the nine comparisons considered. For this example, the average reduction of the pitch rate TE STD is 20%, and the average reduction of the maximum TE error is 11%.

https://doi.org/10.1017/S0001924000001925 Published online by Cambridge University Press

Table 8
Comparison of NLDI-only and NLDI+NN control laws based on flight data – pitch channel

NLDI only→ NLDI+NN ↓	Case #1	Case #2	Case #3	Case #1	Case #2	Case #3
		STD reduction [%]			Max TE reduction [%]	
Case #1	6	20	–12	25	34	–3
Case #2	23	42	2	–1	15	–1
Case #3	35	49	15	4	24	4

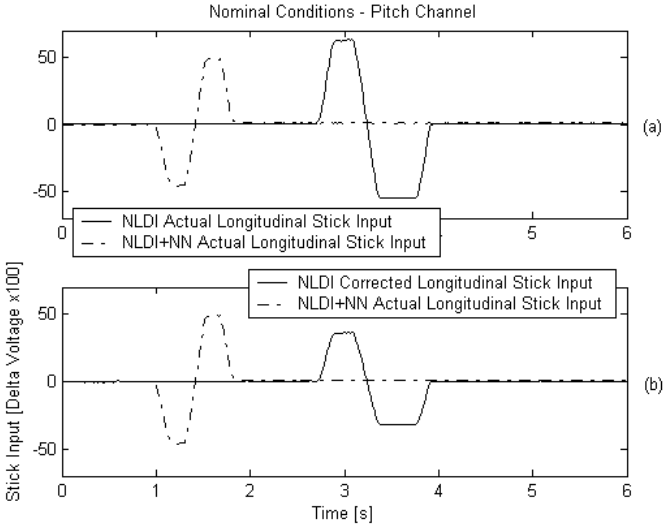


Figure 6. Equivalent longitudinal pilot input.

8.0 CONCLUSIONS

A data reduction algorithm was developed to address issues related to inconsistent test conditions for the performance comparison of different flight control laws within a specific class on a reduced size remotely piloted research aircraft.

Correction algorithms for the angular rate measurements were formulated to account for non-homogeneous atmospheric conditions and similar but not identical pilot inputs. The corrections were determined to ensure identical standard deviations of the perturbations attributed to atmospheric turbulence and identical integral of the absolute value of the pilot input for both data sets involved in a comparison.

The approach was verified using numerical simulations with different levels of atmospheric turbulence and doublet inputs of varying magnitude and duration. The methodology was applied to compute evaluation parameters defined in terms of the standard deviation, integral, and maximum absolute value of the angular rate tracking errors. The proposed data reduction methodology was shown to have overall very high success rates in reducing the negative effects of inconstant test conditions.

The application of the data reduction algorithm was illustrated using flight data for the WVU YF-22 model aircraft for the assessment of neural network augmentation effects on adaptive flight control laws based on non-linear dynamic inversion.

REFERENCES

1. OLSON W.M. *Aircraft Performance Flight Testing*, June 2003, Technical information handbook, Air Force Flight Test Center, CA, USA.
2. KIMBERLIN R.D. *Flight Testing of Fixed-Wing Aircraft*, 2003, AIAA Education Series.
3. US Department of Defense, Military specification – flying qualities of piloted airplanes, 1980, MIL-F8785C.
4. WAN, S., CAMPA, G., YU, G., SEANOR, B., GURURAJAN, S. and NAPOLITANO, M.R. Development of formation control laws for the WVU YF-22 aircraft models, 2003, American Control Conference, 4-6 June 2003, Denver, CO, USA.
5. SEANOR, B., CAMPA, G., GU, Y., NAPOLITANO, M.R., ROWE, L. and PERHINSCHI, M.G. Formation Flight Test Results for UAV Research Aircraft Models, 2004, AIAA2004-6251, AIAA Intelligent Systems Technical Conference, Chicago, IL, USA.
6. PERHINSCHI, M.G., NAPOLITANO, M.R., CAMPA, G., SEANOR, B. and GURURAJAN, S. Design of intelligent flight control laws for the WVU F-22 model aircraft, 2004, AIAA2004-6282, AIAA Intelligent Systems Technical Conference, Chicago, IL, USA.
7. TISCHLER, M.B. (Ed) *Advances in Aircraft Flight Control*, 1996, CRC Press.
8. DUDA, H., BOUWER, G., BAUSCHAT, J.M. and HAHN, K.U. A review of the model following control approach, *Robust Flight Control – A Design Challenge Lecture Notes in Control and Information Sciences*, 1997, pp 116 - 124, Springer-Verlag, London, UK.
9. CALISE, A.J. and SHARMA, M. Adaptive autopilot design for guided munitions, *AIAA J Guidance, Control and Dynamics*, 2000, **23**, (5).
10. KANESHIGE, J., BULL, J. and TOTAH, J.J. Generic neural flight control and autopilot system, August 2000, AIAA Paper 00-4281, Denver, CO, USA.
11. DEETS, D.A. AND EDWARDS, J.W. A remotely augmented vehicle approach to flight testing RPV control systems, November 1974, NASA TM X-56029, NASA Flight Research Center Edwards, CA, USA.
12. DEL FRATE, J.H. and COSENTINO, G.B. Recent flight test experience with uninhabited aerial vehicles at the NASA Dryden Flight Research Center, April 1998, NASA/TM-1998-206546, Dryden Flight Research Center Edwards, CA, USA.
13. Anon, Military specification, Flying qualities of piloted airplanes, November 1990, MILF-STD-1797A, US Department of Defense.
14. PERHINSCHI, M.G., NAPOLITANO, M.R., GURURAJAN, S., SEANOR, B. and BURKEN, J. Data reduction issues for performance evaluation and comparison of flight control laws, 2006, AIAA Atmospheric Flight Mechanics Conference, Keystone, CO, USA.
15. PERHINSCHI, M.G., NAPOLITANO, M.R., CAMPA, G. and FRAVOLINI, M.L. A simulation environment for testing and research of neurally augmented fault tolerant control laws based on non-linear dynamic inversion, 2004, AIAA Modeling and Simulation Technologies Conference, Providence, RI, USA.
16. PERHINSCHI, M.G. and NAPOLITANO, M.R. Analysis of neural augmentation performance for fault tolerant control laws based on flight tests, August 2007, AIAA Guidance, Navigation and Control Conference, Hilton Head, SC, USA.

https://doi.org/10.1017/S0001924000001925 Published online by Cambridge University Press